Proceedings of the 17th World Congress
The International Federation of Automatic Control
Seoul, Korea, July 6-11, 2008

Time-Varying Feedback Control of an Unmanned Autonomous Industrial Forklift

Tua Agustinus Tamba*, Keum-Shik Hong*, and Harijono A. Tjokronegoro**

** School of Mechanical Engineering, Pusan National University; San 30 Jangjeon-dong Gumjeong-gu, Busan, 609-735, Korea.(Tel.: +82-51-510-{1481, 2454}; Fax: +82-51-514-0685; e-mails:{tua_tamba, kshong}@pusan.ac.kr)*

*** Faculty of Industrial Technology (Engineering Physics), Bandung Institute of Technology, Indonesia*

Abstract: In this paper, the development of an unmanned autonomous forklift is discussed. A control architecture using vision, laser ranger finder, sonar, etc. for autonomous navigation is presented. The kinematics of a spin-turn mechanism is analyzed first, and then the obtained kinematics equations are transformed to the equations represented by path variables. These equations are nonlinear state equations to be used for control purpose. A time varying feedback control law via the chained form of Murray and Sastry (1993) is derived. The effectiveness of the proposed control law is examined through simulation.

1. INTRODUCTION

The demand toward a higher level of automation has changed the way that today's warehouses and distribution centers operate. An ordinary industrial or warehouse forklift operated by human needs to be refined to achieve an efficient automated industrial task in material handling process, while at the same time increasing the safety of the operation condition. With the fast advances in sensor and computer technology available now, the opportunities for developing an autonomous forklift are immense. This paper discusses a control architecture and a path-following control algorithm for the development of an unmanned autonomous forklift**.**

In recent years, there have been an increasing number of researches on the subject of unmanned vehicle navigation. Particularly, for the development of automatic industrial forklift, several research results can be found (Garibotto et al., 1997; Lecking et al., 2006; Rodríguez et al., 1998; Seelinger and Yoder, 2006). The works presented in Garibotto et al. (1997) and Seelinger and Yoder (2006) describe the development of pallet engagement algorithm by using a vision system, while a different approach for localization and picking up the pallet by using a laser scanner is presented in Lecking et al. (2006). An extensive description for automating an industrial forklift together with a road-following control algorithm by using a camera is presented in Rodríguez et al. (1998).

This paper focuses on the development of a feedback path following controller for an unmanned autonomous forklift based on the kinematics model of the forklift. A control architecture for unmanned forklift based on a number of sensors (4 LRFs, 1 camera, 12 sonars, etc.) is also presented. The aim of the proposed feedback control algorithm is to force the forklift to follow a reference path trajectory provided by a path planner. To build such a controller, a representation of the forklift kinematics in the form of the reference path variable is derived. The contributions of this paper are the following. A control architecture for development of an unmanned industrial forklift by using vision, LRFs, sonar, encoders, gyros, etc. is firstly introduced. A kinematics model for the forklift with spin-turn mechanism is then presented. A feedback control for the kinematics model of the forklift in path variables is also derived.

This paper is structured as follows: In Section 2, a control architecture for the development of an unmanned autonomous industrial forklift is presented. The kinematics of forklift in the inertia frame and its representation in path variables is analyzed in Section 3. In Section 4, a feedback control law that makes the radial and orientation errors of the forklift from the reference path tend to zero is derived. In Section 5, simulation results are provided. Conclusions are given in Section 6.

2. CONTROL ARCHITECTURE

The vehicle to be automated in this paper is a standard industrial forklift CRX-10 produced by CLARK company, which is depicted in Fig. 1. The forklift body is mounted on four wheels: two caster wheels at the front side and one small caster wheel at the right rear without any abilities of steering or traction, and one wheel at the left rear which is used for driving and steering the forklift (see Fig. 3). The dimensions (length x width x height) of the forklift is 2680mm x 1170mm x 2260mm, and its velocity is limited up to 10kph both for empty and loaded operations. To achieve the autonomy, some modifications will be made on the forklift to attach all the necessary sensors and electronic controller of the steering and driving motors (Rodríguez et al., 1998).

For the purpose of localization, a sensor fusion method consisting of internal and external sensors is used to calculate the absolute and relative positions of the forklift.

The internal sensors including encoders, gyros, and height sensors provide direct measurements of the forklift variables, while the external sensors including sonar, LRF, and vision camera provide the relationship between the autonomous forklift and its environment. GPS and gyro sensor are used to calculate the absolute position of the forklift in the global reference frame. To calculate the present position and velocity of the forklift from an initial point (dead reckoning), encoder and gyro sensors are attached on the forklift wheels.

The motion planning task is responsible to execute the actions that lead the forklift to its final destination position. Such a task can be divided into two subtasks: a global motion planning that provides the path to the goal position, and a local motion planning that provides necessary actions to avoid obstacles.

A path following control algorithm is developed for guiding the autonomous forklift along the predetermined path provided by the path-planner, while the LRFs are attached both in front and back sides of the forklift to detect the presence of any obstacle. The control architecture of the unmanned forklift based on several sensors is depicted in Fig. 2. For the development of a true autonomy of the unmanned forklift, a reliable path-following control algorithm that generates consistent behaviors of the vehicle when negotiating a predetermined path is an absolute necessity.

3. FORKLIFT KINEMATICS

3.1 Kinematics in the inertial frame

In Fig. 3, let *O-X-Y* and *o-x-y* be the inertia frame and the body coordinate frame attached to the forklift, respectively. Let v and θ be the velocity of the forklift in the *x*-direction

Sensors	Numbers
LRFs	4
Camera	3
Ultrasonic	10
Encoder	3
Gyros	1
Height sensor	1

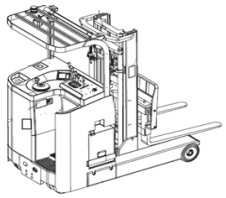

Fig. 1. Sensors to be used in automating an industrial forklift.

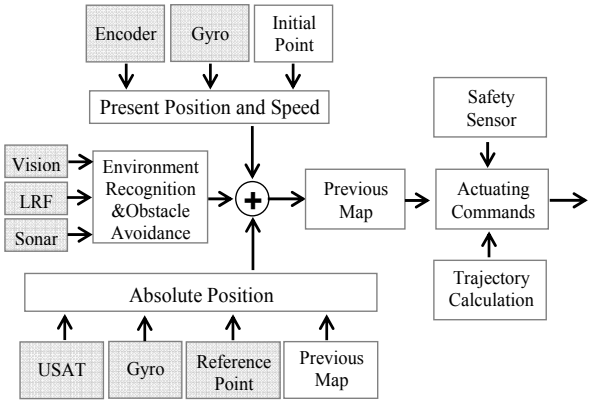

Fig. 2. Control architecture.

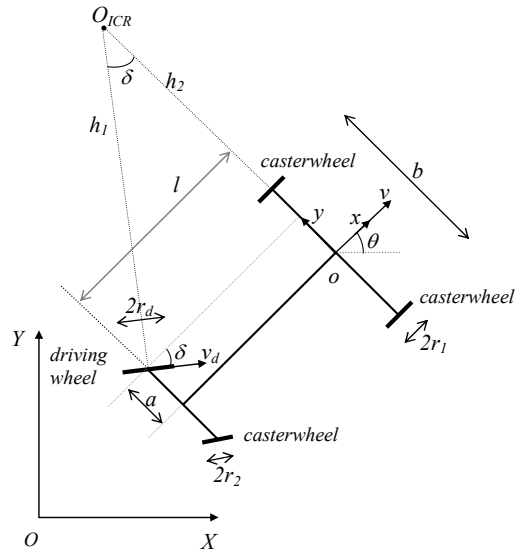

Fig. 3. Schematic of the forklift with a spin-turn steering mechanism.

and the rotational angle of the *x*-axis with respect to the *X*-axis. Let δ be the steering angle of the driving wheel. Under the assumption that the wheels do not slip, let O_{ICR} be the instantaneous center of rotation of the forklift. Finally, let l and a be the length of the forklift and the offset of the center of the driving wheel from the centerline of the body, respectively.

Using the geometry in Fig. 3, the distance between O_{ICR} to the center of the driving wheel becomes

$$h_1 = \frac{l}{\sin\delta}. \tag{1}$$

Then, under the assumption that there is no slippage, the following relationship can be derived.

$$\dot{\delta} = \frac{v_d}{h_1} = \frac{v}{h_1\cos\delta + a} \tag{2}$$

where v_d is the velocity of the driving wheel with the following relationship

$$v_d = r_d\omega_d, \tag{3}$$

where r_d is the radius of the driving wheel, and ω_d is the angular velocity of the driving wheel, respectively. Therefore, the linear velocity of the forklift becomes

$$v = r_d\omega_d\left(\cos\delta + \frac{a\sin\delta}{l}\right). \tag{4}$$

Finally, the kinematics relationship between two input variables $\{\omega_d, \dot{\delta}\}$, where $\dot{\delta}$ is the rate of change of the

steering angle, and three generalized variables $\{X, Y, \theta\}$ (or two output variables $\{v, \dot{\theta}\}$) becomes

$$\begin{aligned}
\dot{X} &= v\cos\theta = r_d\omega_d\left(\cos\delta + \frac{a\sin\delta}{l}\right)\cos\theta, \\
\dot{Y} &= v\sin\theta = r_d\omega_d\left(\cos\delta + \frac{a\sin\delta}{l}\right)\sin\theta, \\
\dot{\theta} &= \frac{r_d\omega_d\sin\delta}{l}.
\end{aligned} \tag{5}$$

3.2 Kinematics in the path coordinates

Fig. 4 shows the position and orientation errors between the actual path and the desired path to be followed by the forklift.

Let $s(x_d(t), y_d(t))$ be the desired path to be followed by the forklift, and the distance along the path is parameterized with $s(t)$. The following relationship can be obtained for $s(t)$

$$s(t) = \int_0^t v_d(\tau)d\tau + s(0), \tag{6}$$

where $s(0)$ is the initial distance along the path and

$$v_d(t) = \sqrt{\dot{x}_d^2(t) + \dot{y}_d^2(t)} \tag{7}$$

is the linear velocity of a projected point of the origin of the body coordinate, *o*, on the path *s*. Let *d* denotes the lateral distance between the forklift reference point, *o*, and the reference path to be followed. Let the positive sign of *d* represent the position of the reference path is on the right-hand side of the forklift and the negative sign of *d* represent the position of the reference path is on the left-hand side of the forklift. Let θ_e denote the orientation error of the forklift with respect to the reference path which can be defined as follows:

$$\theta_e = \theta - \theta_d \tag{8}$$

where θ_d denotes the desired orientation of the forklift, which is tangent to the desired path, *s*. Based on Fig. 4, the curvature for any given point on the reference path at each instant time can be drawn as follows (John and Nelson, 1989).

$$c(s) = \frac{d\theta_d}{ds} = \frac{d\theta_d}{dt}\frac{dt}{ds} = \frac{\dot{\theta}_d(t)}{\dot{s}(t)}. \tag{9}$$

The representation of the reference path in path variables $\{s, d, \dot{\theta}_e\}$ can be derived as follows.

$$\begin{aligned}
\dot{s} &= v\cos\theta_e + d(t)\dot{\theta}_d(t) \\
&= v\cos\theta_e + d(t)c(s)\dot{s}(t),
\end{aligned}$$

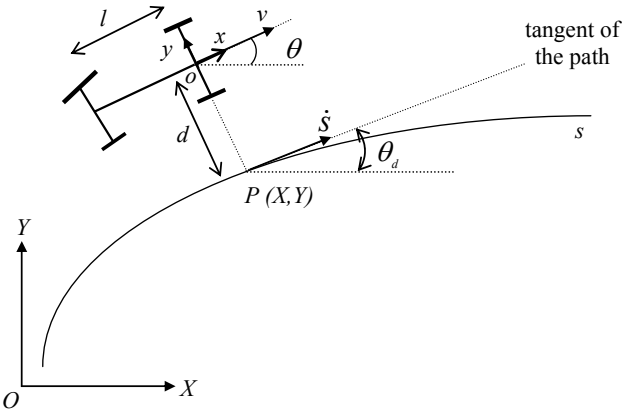

Fig. 4. Kinematics model of the forklift in the path variables.

$$\begin{aligned}
\dot{s}(t) &= \frac{v\cos\theta_e}{[1 - d(t)c(s)]}, \\
\dot{d} &= v\sin\theta_e, \\
\dot{\theta}_e &= \dot{\theta}(t) - \dot{\theta}_d(t) = \dot{\theta}(t) - c(s)\dot{s}(t).
\end{aligned} \tag{10}$$

The substitution of (4) into (10) results in the following equations

$$\begin{aligned}
\dot{s}(t) &= \frac{v_d\cos\theta_e\left(\cos\delta + \frac{a\sin\delta}{l}\right)}{[1 - d(t)c(s)]}, \\
\dot{d}(t) &= v_d\sin\theta_e(t)\left[\cos\delta + \frac{a\sin\delta}{l}\right], \\
\dot{\theta}_e(t) &= \frac{v_d\sin\delta}{l} - \frac{v_d c(s)\cos\theta_e\left(\cos\delta + \frac{a\sin\delta}{l}\right)}{[1 - d(t)c(s)]}, \\
\dot{\delta}(t) &= \omega_s,
\end{aligned} \tag{11}$$

where ω_s is the steering angular velocity. Since the inputs to the forklift system are v_d and ω_s, (11) can be rewritten in the following compact form

$$\begin{bmatrix} \dot{s} \\ \dot{d} \\ \dot{\theta}_e \\ \dot{\delta} \end{bmatrix} = \begin{bmatrix} \frac{\cos\theta_e\left(\cos\delta + \frac{a\sin\delta}{l}\right)}{[1 - d(t)c(s)]} \\ \sin\theta_e\left(\cos\delta + \frac{a\sin\delta}{l}\right) \\ \frac{\sin\delta}{l} - \frac{c(s)\cos\theta_e\left(\cos\delta + \frac{a\sin\delta}{l}\right)}{[1 - d(t)c(s)]} \\ 0 \end{bmatrix} v_d + \begin{bmatrix} 0 \\ 0 \\ 0 \\ 1 \end{bmatrix} \omega_s \tag{12}$$

where v_d and ω_s denote the linear and angular velocities of the forklift driving wheel, respectively. It can be seen that (12) is a nonlinear system with four state variables ($\dot{s}, \dot{d}, \dot{\theta}_e$, and $\dot{\delta}$) and two input variables (v_d and ω_s).

4. CONTROL LAW DESIGN

The control objective in this paper is to design a controller that will drive the lateral error d and orientation error θ_e in (12) to zero, so that the forklift can follow the desired trajectory. In order to design such a controller, a new coordinate transformation called the chained form is applied to model (12), which was introduced by Murray and Sastry (1993). This section will describe the coordinate transformation of model (12) into the chained form, and then derive a feedback control law using the obtained chained form.

4.1 Coordinates transformation in chained form

The chained form is one of the canonical structures for the kinematics model of a nonholonomic system. This model is very useful because it provides the system a very controllable structure for the systematic development of the control strategy.

The chained form for a system with 2 input variables and n state variables can be written as a (2, n) chained form model with the following form (Murray and Sastry, 1993)

$$\begin{aligned} \dot{x}_1 &= u_1, \\ \dot{x}_2 &= u_2, \\ \dot{x}_3 &= x_2 u_1, \\ \dot{x}_n &= x_{n-1} u_1. \end{aligned} \tag{13}$$

Although the chained form in (13) is nonlinear, it has also a strong underlying linear structure. Based on the path coordinate model derived in the previous section, the forklift studied in this paper has four state variables. Therefore the chained form for the forklift path coordinate (12) can be described in the following (2, 4) chained form

$$\begin{aligned} \dot{x}_1 &= u_1, \\ \dot{x}_2 &= u_2, \\ \dot{x}_3 &= x_2 u_1, \\ \dot{x}_4 &= x_3 u_1. \end{aligned} \tag{14}$$

The transformation of the state variables is then given as

$$\begin{aligned} x_1 &= s, \\ x_2 &= -c'(s) d(t) \tan\theta_e - \frac{c(s)\left[1 - d(t)c(s)\right]\left[1 - \sin^2\theta_e\right]}{\cos^2\theta_e} \\ &\quad - \frac{\sin\delta\left[1 - d(t)c(s)\right]^2}{\cos^3\theta_e\left[l\cos\delta + a\sin\delta\right]}, \\ x_3 &= \tan\theta_e\left[1 - d(t)c(s)\right], \\ x_4 &= d, \end{aligned} \tag{15}$$

where $c'(s)$ is the derivation of path curvature $c(s)$ with respect to s. The inputs of the chained form then

$$\begin{aligned} v_d &= \frac{1 - d(t)c(s)}{\cos\theta_e\left(\cos\delta + \dfrac{a\sin\delta}{l}\right)} u_1, \\ \omega_s &= \alpha_2(q)\left[u_2 - \alpha_1(q)u_1\right], \end{aligned} \tag{16}$$

where v_d is the linear velocity and ω_s is angular velocity, respectively, of the driving wheel, and

$$\begin{aligned} \alpha_1(q) &= \frac{\partial x_2}{\partial s} + \frac{\partial x_2}{\partial d}\left[1 - d(t)c(s)\right]\tan\theta_e \\ &\quad + \frac{\sin\delta\left[1 - d(t)c(s)\right]}{l\cos\theta_e\left(\cos\delta + \dfrac{a\sin\delta}{l}\right)}, \\ \alpha_2(q) &= \frac{\cos^3\theta_e\left(l\cos\delta + a\sin\delta\right)}{l\left[1 - d(t)c(s)\right]}. \end{aligned} \tag{17}$$

4.2 A time varying feedback control law

The control design via smooth time varying feedback presented in this paper is based on the work presented in Schowerer (2005) and Samson et al. (2004). This paper presents a modification of their work for the development of path following controller by using the chained form of the path coordinate model (12). In this form, controller drives x_2 and x_4 in (14) to zero.

For a system given in the chain form, its variables can be rearranged as

$$\chi = (x_1, x_2, \ldots, x_{n-1}, x_n) = (x_1, x_n, \ldots, x_3, x_2). \tag{18}$$

Rearranging the chained form (14) in structure of (18), the following new chained form can be obtained.

$$\dot{\chi} = h_1(\chi)u_1 + h_2 u_2,\ h_1(\chi) = \begin{bmatrix} 1 \\ \chi_2 \\ \vdots \\ \chi_n \\ 0 \end{bmatrix}, h_2(\chi) = \begin{bmatrix} 0 \\ 0 \\ 0 \\ \vdots \\ 1 \end{bmatrix}. \tag{19}$$

For the forklift kinematics model, the above reordering is an exchange between the second and fourth coordinates. Let $\chi = h_1(x_1, \chi_2)$, where $\chi_2 = (x_2, x_3, \ldots, x_n)$, the chained form (19) can be rewritten in the following structure.

$$\begin{aligned} \dot{\tilde{x}}_1 &= 0, \\ \dot{\chi}_2 &= \begin{bmatrix} \dot{x}_2 \\ \dot{x}_3 \\ \dot{x}_4 \end{bmatrix} = \begin{bmatrix} 0 & u_1(t) & 0 \\ 0 & 0 & u_1(t) \\ 0 & 0 & 0 \end{bmatrix}\begin{bmatrix} x_2 \\ x_3 \\ x_4 \end{bmatrix} + \begin{bmatrix} 0 \\ 0 \\ 1 \end{bmatrix} u_2, \end{aligned} \tag{20}$$

where $\tilde{\chi}_1 = \chi_1 - \int_0^t u_1(\tau)d\tau$.

The structure χ_2 in (20) is similar to the controllable canonical form for the linear system. If u_1 is constant and nonzero, the second part in (20) is clearly controllable. If x_1 is assumed to vary monotonically with time, then the differentiation with respect to time can be replaced by differentiation with respect to χ_1 as shown below

$$\frac{d}{dt} = \frac{d}{d\chi_1}\dot{\chi}_1 = \frac{d}{d\chi_1}u_1$$
$$sign(u_1)\frac{d}{d\chi_1} = \frac{1}{|u_1|}\cdot\frac{d}{dt}. \quad (21)$$

With the change of variable in u_1, then variables $\dot{x}_2, \dot{x}_3,$ and $\dot{x}_4$ in (20) can be rewritten as

$$\chi_2^{[1]} = sign(u_1)\chi_2,$$
$$\chi_3^{[1]} = sign(u_1)\chi_3, \quad (22)$$
$$\chi_4^{[1]} = sign(u_1)u_2',$$

where

$$\chi_i^{[j]} = sign(u_1)\frac{d^j\chi_i}{d\chi_i^j} \text{ and } u_2' = \frac{u_2}{u_1}.$$

The relationship in (22) is a controllable linear time-invariant system that admits an exponentially stable linear feedback in the following form (Laumound, 1998)

$$u_2'(\chi_2) = -sign(u_1)^{n-1}\sum_{i=1}^{n-1} k_i\chi_2^{[i-1]}. \quad (23)$$

Hence the time-varying control can be calculated as

$$u_2(\chi_2, t) = u_1(t)u_2'(\chi_2). \quad (24)$$

For the chained form of the forklift in (14), the stable and controllable linear feedback form is given by

$$u_2'(\chi_2, \chi_3, \chi_4) = -sign(u_1)[k_1\chi_2 + k_2 sign(u_1)\chi_3 + k_3\chi_4] \quad (25)$$

and the linear path following feedback control law becomes

$$u_2(\chi_2, \chi_3, \chi_4, t) = -k_1|u_1(t)|\chi_2 - k_2u_1(t)\chi - k_3|u_1(t)|\chi_4. \quad (26)$$

Finally, in rewriting (16) by using the measured variables and errors, they become

$$v_d = \frac{[1 - d(t)c(s)]u_1}{\cos\theta_e\left(\cos\delta + \frac{a\sin\delta}{l}\right)},$$

$$\omega_s = -\alpha_2(q)u_1[-k_1\chi_2 - k_2\chi_3 - k_3|u_1(t)|\chi_4 - \alpha_1(q)], \quad (27)$$

where (α_1, α_2) and (χ_2, χ_3, χ_4) are defined in (17) and (18), respectively.

5. SIMULATION

This section describes the simulation for the application of the control algorithm derived in Section 3 for the path following control of the forklift. For simplicity, the reference path is described by a circle with a radius of 5 meters. With this circular reference path, the magnitude of the trajectory is

$$c(s) = \frac{1}{r}$$

where r is the radius of the circle. Since the curvature of the reference path is constant, then its time derivative can be assumed equal to zero.

The initial position of the forklift is set to $(x, y, \theta) = (0, 2.25, 135°)$, which gives the initial lateral error, d of 0.25 meters, and initial orientation error, θ_e of 45°. The linear velocity of the forklift is set to 1 m/s, and the gains for the feedback controller are set to $(k_1, k_2, k_3) = (10, 10, 10)$.

The simulation results for the path following control is given in Fig. 5, for which u_1 and u_2 are depicted in Fig. 6, and actual control inputs v_d and ω_s are depicted in Fig. 7 and Fig. 8, respectively. The lateral error d and orientation error θ_e shown in Fig. 9 and Fig. 10, respectively, show that the proposed feedback controller makes the radial and orientation errors tend to zero, thus forces the forklift to follow the predetermined path.

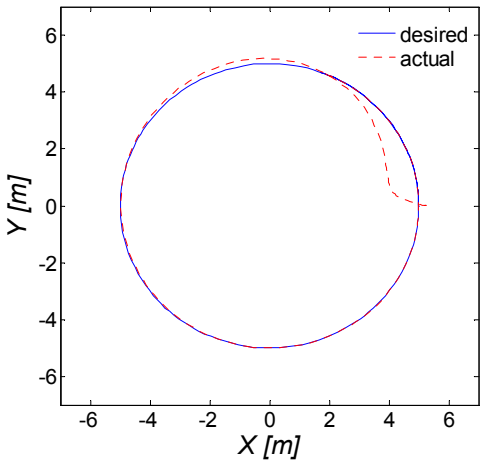

Fig. 5. Simulation for a circular desired trajectory.

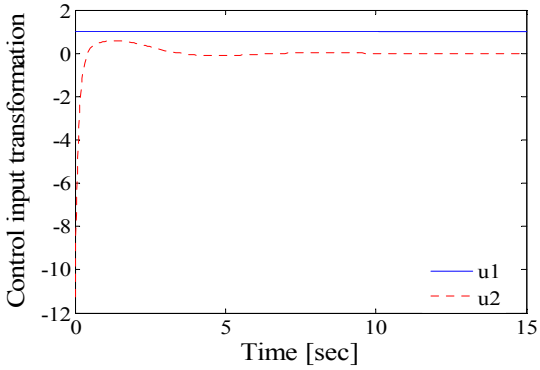

Fig. 6. Control inputs u_1 and u_2.

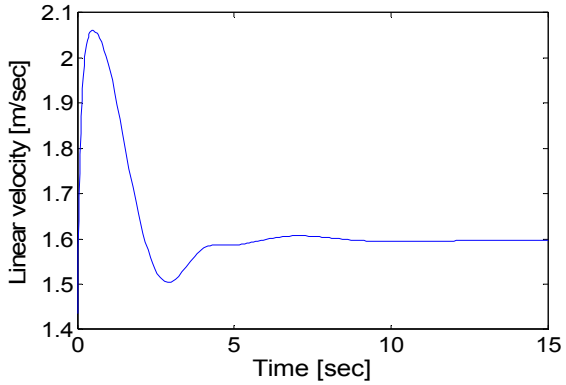

Fig. 7. Linear velocity v_d of the steering wheel.

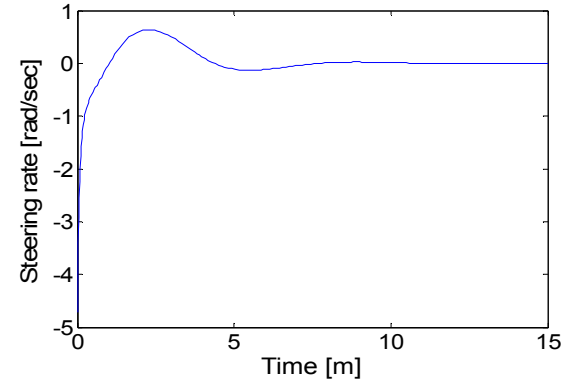

Fig. 8. Angular velocity ω_s of the steering wheel.

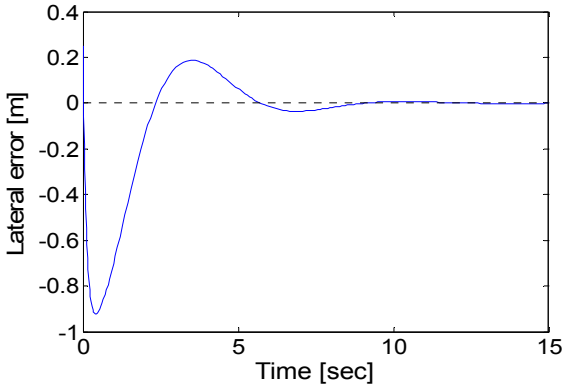

Fig. 9. Lateral error between the forklift and the desired path.

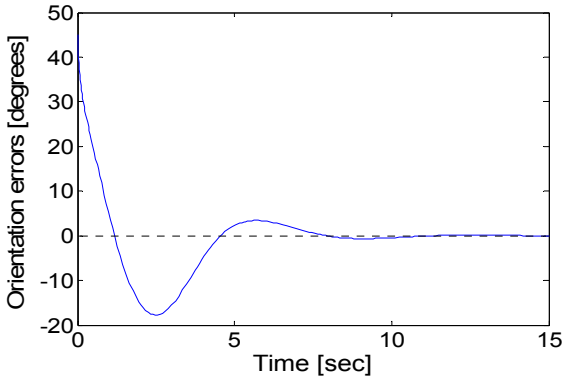

Fig. 10. Orientation error between the forklift and the desired path.

6. CONCLUSION

Control architecture for the development of an unmanned autonomous forklift is presented in this paper. For the purpose of path following control, a time varying feedback control algorithm was derived and implemented to the kinematics model of the forklift. From the simulation results, it can be seen that the proposed feedback controller makes the lateral and orientation errors of the forklift with respect to a given path tend to zero.

ACKNOWLEDGMENT

This work was supported by the Regional Research Universities Program (Research Center for Logistics Information Technology, LIT) granted by the Ministry of Education & Human Resources Development, Korea.

REFERENCES

Garibotto, G., S. Masciangelo, M. Ilic and P. Bassino (1996). ROBOLIFT: a vision guided autonomous fork-lift for pallet handling. *Proceedings of International Robots and Systems (IROS)*, pp. 656-663.

John, D. and R. D. Nelson (1989). *Dictionary of mathematics*, pp. 81-82. Penguin Books, England.

Laumond, J. P. (1998). *Robot motion planning and control*, Springer-Verlag, Toulouse.

Lecking, D., O. Wulf and B. Wagner (2006). Variable pallet pick-up for automatic guided vehicles in industrial environments. *Proceedings of IEEE Conference on Emerging Technologies and Factory Automation*, pp.1169-1174.

Murray, R. M. and S. S. Sastry (1993). Nonholonomic motion planning: steering using sinusoids. *IEEE Transactions on Automatic Control*, **38** (5), pp. 700-716.

Rodríguez, F. J., M. Mazo and M. A. Sotelo (1998). Automation of an industrial forklift truck, guided by artificial vision in open environment. *Autonomous Robot*, **5** (2), pp. 215-231.

Samson, C., A. De Luca and G. Oriolo (2004). *Feedback control of a nonholonomic car-like robot*. Dipartimento di Informatica e Sistemistica, Università di Roma "La Sapienza".

Schworer, I. (2005). Navigation and control of autonomous vehicle. *MS Thesis, Virginia Polytechniq Institute and State University*.

Seelinger, M. and J. D. Yoder (2006). Automatic visual guidance of a forklift engaging a pallet. *Robotics and Autonomous System*, **54** (12), pp. 1026-1038.